

DOI: 10.1002/chem.201301150

Validity of Inorganic Nanosheets as an Efficient Planar Substituent To Enhance the Enantioselectivity of Transition-Metal-Catalyzed Asymmetric Synthesis

Li-Wei Zhao, Hui-Min Shi, Zhe An, Jiu-Zhao Wang, and Jing He*^[a]

Abstract: Effectively enhancing the enantioselectivity is a persistent challenge in heterogeneous asymmetric catalysis. Here, the validity of a layered double hydroxides (LDH) nanosheet as an efficient planar substituent to enhance the enantioselectivity has been investigated theoretically; first in vanadium-catalyzed asymmetric epoxidation of allylic alcohols, and then in zinc-catalyzed direct asymmetric aldol addition. The computational predication is further confirmed experimentally in zinc-catalyzed direct asymmetric aldol addition by controlling the location of catalytic sites.

Keywords: asymmetric catalysis · density functional calculations · enantioselectivity · heterogeneous catalysis · nanosheets

Introduction

Heterogeneous asymmetric catalysis is considered as an environmentally friendly chemical process to produce chiral compounds, and has been greatly stimulated by the growing demand for optically pure compounds in chemical and pharmaceutical industries.^[1–3] But binding a homogeneous catalyst to solid surfaces usually leads to deteriorated activity^[4] and enantioselectivity,^[5–8] or even complete elimination of enantioselectivity.^[9,10] A lot of attempts have been reported to improve the enantioselectivity of heterogeneous catalysis. Confinement of metal complexes^[11–15] and/or metal-free organocatalyst^[16–18] in the channels or mesopores was found to be able to enhance the enantiomer excess (*ee*) or at least retain the enantioselective level of homogeneous counterparts. Intercalation of active centers into the interlayer regions of layered compounds, layered double hydroxides (LDHs)^[19] or laponite,^[20,21] for example, was also reported to be able to retain or improve the enantioselectivity. A moderate *ee* value has been achieved by this approach even in the case that the homogeneous counterpart could only afford racemic products.^[22]

In our recent research,^[23] it was revealed in the vanadium-catalyzed asymmetric epoxidation of allylic alcohols by using nanosheet-attached α -amino acid anions as chiral ligands that the enantioselectivity improvement was retained after elimination of interlayer confinement by delamination of ligand-intercalated LDHs. Further investigation^[24] indicated that the increment of enantioselectivity displayed a

close relationship to the location of vanadium centers. When the vanadium centers were coordinated with the amino acid anions situated at the center of LDH interlayer regions, a remarkable *ee* increment was observed (from 56 to 91% *ee* for the *trans* isomers and from 26 to 68% *ee* for the *cis* isomers). When the vanadium centers were coordinated with amino acid anions situated at the edges of LDH interlayer regions, a moderate *ee* increment was observed (to 80% *ee* for the *trans* isomers and 9% *ee* for the *cis* isomers). In this case, the LDH layers themselves as 2D nanosheets are proposed to act as a planar substituent of α -amino acid ligand in improving the enantioselectivity probably through either steric resistance or multiple interactions. This work investigates theoretically the validity of LDH nanosheet as an efficient planar substituent to enhance enantioselectivity first in the vanadium-catalyzed asymmetric epoxidation of allylic alcohols, and then in the zinc-catalyzed direct asymmetric aldol addition between unmodified ketones and aldehydes, a reaction which is considered to be difficult to achieve satisfactory enantioselectivity.^[25–27] The computational prediction is further confirmed experimentally in zinc-catalyzed direct asymmetric aldol addition by controlling the location of catalytic sites. This work provides valuable insight into the strategy, as well as the applicability and practicability, of designing efficient catalysts in enantioselective catalysis and asymmetric synthesis.

Results and Discussion

Theoretical prediction of the validity of inorganic nanosheet as an efficient planar substituent: In the intercalate structure,^[24] the carboxylic protons of α -amino acids are replaced by positively charged LDH layers. Then, the interlayer α -amino acid anions bear “huge” and “rigid” nanosheets, instead of single atoms. Especially when the vanadium centers

[a] L.-W. Zhao, H.-M. Shi, Z. An, J.-Z. Wang, Prof. J. He
State Key Laboratory of Chemical Resource Engineering
Beijing University of Chemical Technology
Box 98, 15 Beisanhuan Dong Lu
Beijing 100029 (P.R. China)
Fax: (+86)10-64425385
E-mail: jinghe@263.net.cn

are coordinated with the α -amino acid anions situated at the inner interlayer regions (Figure 1), the LDH layer as the substituent of α -amino acid ligand displays plane-symmetry. Qualitatively, the uniform chiral environment provided by

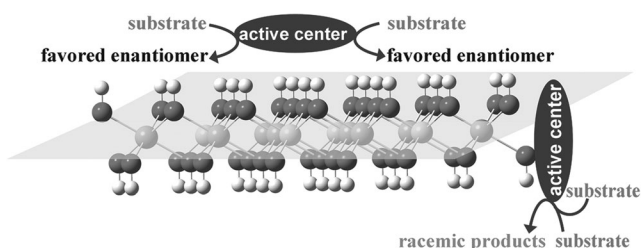


Figure 1. Schematic illustration of the LDH layer as a substituent displaying plane-symmetry.

nanosheet-modified α -amino acid is able to favor the formation of one transition state, thereby enhancing chiral induction. In addition to the electrostatic interactions between positively charged layers and interlayer α -amino acid anions, two H-bonds (C2–O1...H1 and C2–O2...H2) are formed between the hydroxyl groups of LDH layers and the attached α -amino acid anions, which were calculated to be 1.77 and 1.68 Å (Figure 2a). The existence of the H-bonds, a kind of short-range and orientation interaction,^[28] facilitates LDH layers as the substituent of attached α -amino acid anions. After the coordination of vanadium centers to α -amino acid anions, the LDH layer affords a more H-bond with O=V moiety (Figure 2b), which is calculated as 1.80 Å when V centers are located at the inner interlayer regions and 1.70 Å when V centers are located at the edges. The V=O...layer OH bond weakens the H-bonds between LDH layer and α -amino acid anions from 1.77/1.68 Å (C2–O1...H1/C2–O2...H2) to 1.90/1.70 Å and 2.07/1.87 Å, respectively. In accordance, the linkage rigidity between brucite-like layer and attached α -amino acid anions is stronger when V centers are coordinated at the inner interlayer regions.

In the vanadium-catalyzed epoxidation of 2-methyl-cinnamyl alcohol, our previous work^[24] has revealed that when the vanadium centers are coordinated at the inner interlayer regions, the access of 2-methyl-cinnamyl alcohol in its convex conformation to form the (2*S*,3*S*) transition state has to weaken the C2–O1...H1 from 1.90 to 1.95 Å, whereas the access in its concave conformation to form (2*R*,3*R*) well preserves the C2–O1...H1 (from 1.90 to 1.85 Å). That means, the (2*R*,3*R*) transition state is favored whereas (2*S*,3*S*) is inhibited. When the vanadium centers are coordinated at the edges of LDH interlayer regions (Figure 3), the access of 2-methyl-cinnamyl alcohol in its convex conformation weakens C2–O1...H1 from 2.07 to 2.10 Å, whereas concave access strengthens C2–O1...H1 from 2.07 to 2.05 Å. As a result, either the catalytic centers are located at the inner interlayer regions or at the edges, it is easier for (2*R*,3*R*) transition state to be formed, accounting for the *ee* increment in comparison to homogeneous counterpart. In each case C2–

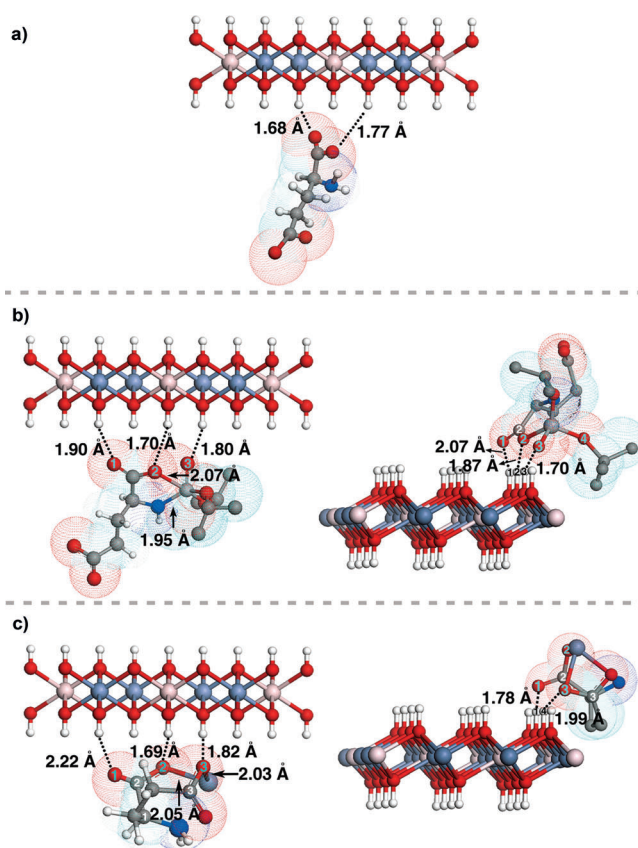


Figure 2. The primary H-bonding distances between a) LDH layer and attached α -amino acid anion; b) LDH layer, attached α -amino acid anion, and vanadium centers coordinated (left) at the inner interlayer region or (right) at edge of interlayer region; c) LDH layer, attached α -amino acid anion, and zinc centers coordinated (left) at the inner interlayer region or (right) at edge of interlayer region (light blue = Zn, pink = Al, dark blue = N, gray = C, white = H).

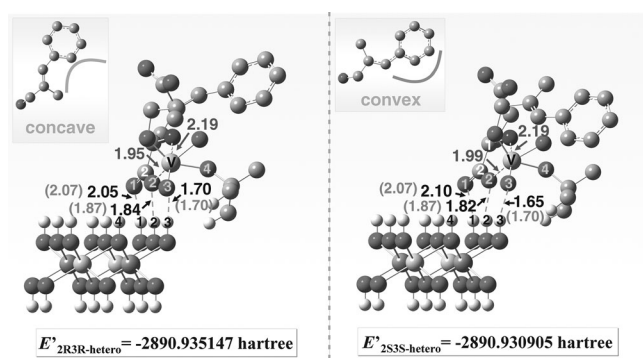


Figure 3. The calculated energies and primary bonding distances for the optimized transition states in the epoxidation of 2-methyl cinnamyl alcohol when the catalytic centers are located at the edges of the interlayer regions.

O2...H2 bonds is strengthened, from 1.70 to 1.61 Å (access in concave conformation) or 1.67 Å (access in convex conformation) when the catalytic centers are located at the inner interlayer regions, and from 1.87 to 1.84 or 1.82 Å when the catalytic centers are located at the edges.

On the other hand, in the (2*R*,3*R*) transition state, the C2–O1...H1 and C2–O2...H2 bonds are calculated to be 1.85 and 1.61 Å when catalytic centers are located at the inner interlayer regions, which are both stronger than those in the (2*S*,3*S*) transition state (1.95 and 1.67 Å). Moreover, a new H-bond is formed between the alcoholic moiety (O4) in 2-methyl-cinnamyl alcohol and the LDH layer, which is also stronger in the (2*R*,3*R*) transition state than in the (2*S*,3*S*) transition state (1.72 versus 1.81 Å). When the catalytic centers are located at the edges of interlayer regions (Figure 3), although the C2–O1...H1 is stronger in the (2*R*,3*R*) transition state than in (2*S*,3*S*) transition state (2.05 vs. 2.10 Å), the C2–O2...H2 is weaker than in (2*S*,3*S*) transition state (1.84 vs. 1.82 Å). In addition, the 2-methyl-cinnamyl alcohol molecules that attack in either concave or convex conformation form no new H-bond with the LDH layer, which decreases the difference in the H-bonding interaction between (2*R*,3*R*) and (2*S*,3*S*) transition states. As a result, the energy difference between (2*R*,3*R*) and (2*S*,3*S*) transition states is 2.94 kJ mol⁻¹ lower when vanadium centers are located at edge than at inner interlayer region, accounting for less increment of the *ee* value when the catalytic centers are located at edge than at inner interlayer region (80 vs. 91% *ee* for *trans* isomers). According to the calculation results based on experimental observations, it is apparent that the efficient enhancement of enantioselective induction originates from the location of catalytic centers at the inner interlayer regions, which supports the rational presumption (Figure 1) of the significance of the plane-symmetry of inorganic nanosheet as the substituent.

On the basis of the results for the vanadium-catalyzed epoxidation, further theoretical prediction is performed on the zinc-catalyzed direct asymmetric aldol addition of cyclohexanone to 4-nitrobenzaldehyde using L-glutamate as chiral ligand. According to the optimized configuration (Figure 2c), both carboxylates of α-amino acid anion afford coordination to Zn, facilitating the formation of an eight-member ring to orient the carboxyl groups to the LDH layer. The H-bonds between LDH layers and attached α-amino acid anions are calculated to be 2.22 (C2–O1...H1), 1.69 (C2–O2...H2), and 1.82 Å (C3–O3...H3) when the Zn centers are coordinated at the inner interlayer regions, whereas they are calculated as 1.78 (C2–O1...H1) and 1.99 (C3–O3...H4) when the Zn centers are coordinated at the edge interlayer regions. Our previous work^[29] has revealed that in the direct aldol addition of cyclohexanone to 4-nitrobenzaldehyde, the Si face attack of aldehyde to *syn*-enolate to form the (2*R*,1'*S*) transition state has to break C2–O2...H2 and C3–O3...H3 bonds when the catalytic centers are located at the inner interlayer regions, whereas the Re face attack of aldehyde to *anti*-enolate to form the (2*S*,1'*R*) transition state well preserves C3–O3...H3 (1.83 vs. 1.82 Å) and only weakens C2–O2...H2 from 1.69 to 2.08 Å. That means, the formation of (2*S*,1'*R*) transition state is favored, whereas (2*R*,1'*S*) is inhibited. In the (2*R*,1'*S*) transition state, the H-bond C3–O3...H4 is formed instead of C3–O3...H3. C3–O3...H4 is calculated to be 2.00 Å, which is weaker than

C3–O3...H3 that is preserved in (2*S*,1'*R*) transition state. Meanwhile, the aldehyde moiety (O6) and nitro moiety (O8) in 4-nitrobenzaldehyde also form H-bonds with LDH layer, which are 2.31 and 2.19 Å in (2*S*,1'*R*) transition state, whereas they are 2.32 and 2.25 Å in (2*R*,1'*S*) transition state. It can be predicted from either the alteration of H-bonds in the substrate access and the difference between the H-bonds in the transition states that LDH layers are to promote *ee* values with (2*S*,1'*R*) as the excess enantiomer.

For the catalytic system in which the catalytic centers are located at the edges of interlayer regions, the Si face attack of aldehyde to the *syn*-enolate to form the (2*R*,1'*S*) transition state strengthens the C2–O1...H1 and C3–O3...H4 from 1.78 and 1.99 Å to 1.74 and 1.91 Å, whereas the Re face attack of aldehyde to *anti*-enolate to form the (2*S*,1'*R*) transition state preserves the C3–O3...H4 but has to weaken C2–O1...H1 to 2.22 Å (Figure 4). That means, it is easier for

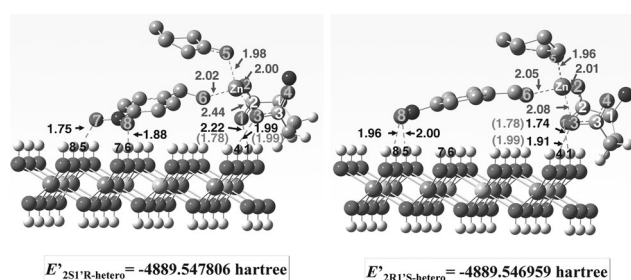


Figure 4. The calculated energies and primary bonding distances for the optimized transition states in the direct asymmetric aldol reaction when the catalytic centers are located at the edges of the interlayer regions.

(2*R*,1'*S*) to be formed than (2*S*,1'*R*) transition state. On the other hand, although, the C2–O1...H1 and C3–O3...H4 are weaker in (2*S*,1'*R*) transition state than in (2*R*,1'*S*) transition state (2.22 and 1.99 Å vs. 1.74 and 1.91 Å), the H-bonds between the nitro moiety (O7 and O8) in 4-nitrobenzaldehyde and LDH layer are calculated to be both stronger in (2*S*,1'*R*) transition state than in (2*R*,1'*S*) transition state (1.75 and 1.88 Å vs. 1.96 and 2.00 Å). That means, (2*S*,1'*R*) is more stable than (2*R*,1'*S*) transition state. The difference between the H-bonds in the transition states is conflict to the alteration of H-bonds in the substrate access, making neither (2*S*,1'*R*) nor (2*R*,1'*S*) isomer favored.

Experimental verification of LDH nanosheets as a valid plane-symmetric substituent to enhance enantioselectivity in zinc-catalyzed direct asymmetric aldol addition:

According to the theoretical prediction, the locations of catalytic centers are altered experimentally, and the relationship between the *ee* value and locations of active centers have then been explored (Figure 5). The dispersion of Zn centers along the 2D interlayer region has been probed by line-scanning energy dispersive spectroscopy (EDS; Figure 5a). The Zn centers are mainly located at the edges of interlayer regions (Figure 5b) using Zn(OAc)₂ as the precursor to coordinate to the L-glutamate-intercalated Zn/Al-LDH. With the Zn

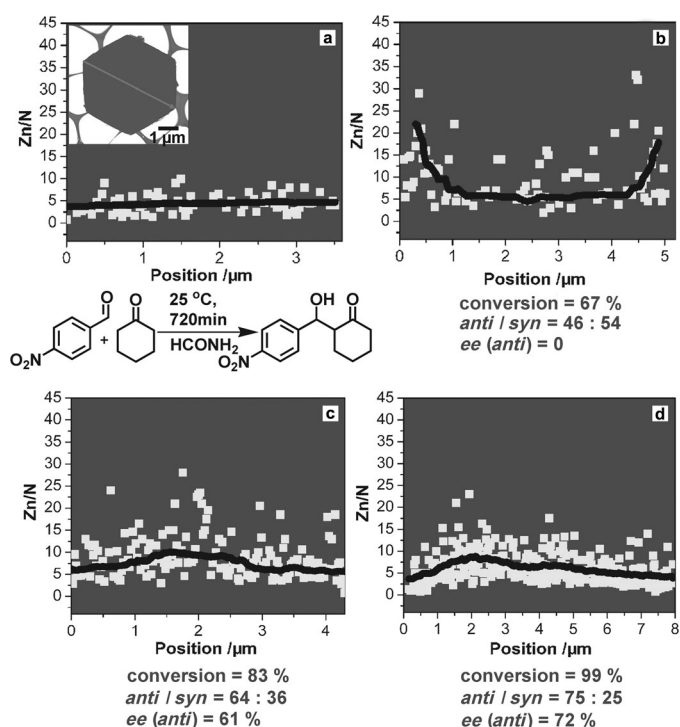


Figure 5. Images of zinc distribution visualized by energy dispersive spectroscopy (EDS) energy profiles and the *ee* values observed with the corresponding catalysts: a) Zn/Al-LDHs intercalated with L-glutamate; the inset indicates the scanning line through the 2D plane for (a)–(d); b) Zn(OAc)₂ as precursor, coordinated with the L-glutamate intercalated between LDH layers; c) Zn(CH₂CH₃)₂ as precursor, coordinated with the L-glutamate intercalated between LDH layers; d) Zn(OAc)₂ as precursor, coordinated with the L-glutamate attached to exfoliated LDH layers. In each case, the uncoordinated zinc moieties were excluded by thorough washing prior to the characterizations.

centers coordinated at the edges as catalytic sites, only racemic products are obtained. By using Zn(CH₂CH₃)₂ as the precursor, the Zn centers are mainly located at the inner interlayer regions (Figure 5c). With the Zn centers coordinated at the inner region, 61% *ee* is afforded for *anti*-isomers with 83% conversion. Exfoliating L-glutamate-intercalated Zn/Al-LDH to make the interlayer ligand more accessible, the Zn centers are coordinated homogeneously with the L-glutamate (Figure 5d) even using Zn(OAc)₂ as the precursor of catalytic site. As a result, 72% *ee* was afforded for *anti*-isomers with 99% conversion. The crucial role of the LDH layer as a planar substituent of attached α -amino acid ligand in the enantioselective improvement has been clearly revealed.

To further confirm the role of LDH layers in the enantioselective boost, the site of catalytic reaction was monitored by using 8-hydroxyquinoline as a tracing molecule. 8-Hydroxyquinoline is similar in size to 4-nitrobenzaldehyde, one of the catalyzed substrate in this work. 8-Hydroxyquinoline can coordinate with the Zn centers that are introduced as catalytic sites and in unsaturated coordination, rather than with the hexa-coordinated Zn in the brucite-like layers. The complex between Zn and 8-hydroxyquinoline emits fluores-

cence under the laser excitation.^[30] As can be seen from Figure 5, the fluorescent images of the location in which 8-hydroxyquinoline coordinated with zinc centers, for the catalyst affording no enantioselectivity, the fluorescent light was much stronger at the edge than the inner interlayer region (Figure 6a), indicating that the catalysis occurred

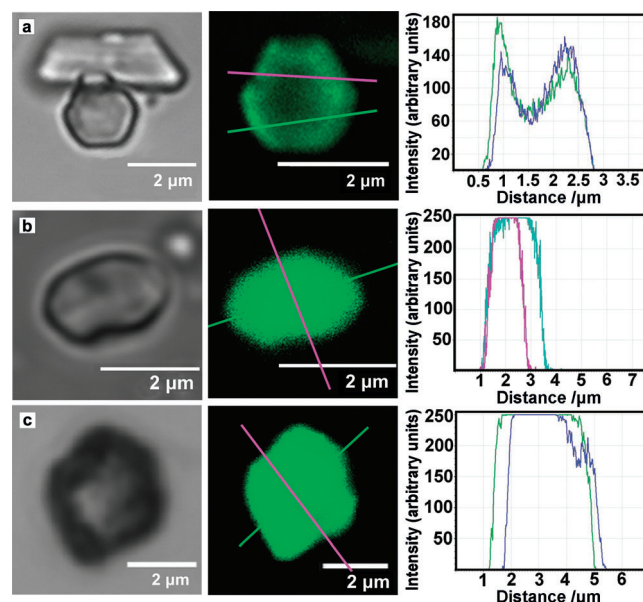


Figure 6. Fluorescent images using 8-hydroxyquinoline as a tracing molecule to monitor the location of catalytic reactions using the catalysts based on a) Zn(OAc)₂ as precursor, coordinated with L-glutamate intercalated LDHs; b) Zn(OAc)₂ as precursor, coordinated to the L-glutamate attached to exfoliated LDH layers; c) Zn(CH₂CH₃)₂ as precursor, coordinated with L-glutamate intercalated LDHs. The catalytic results are also provided to present a clear image of the substituent role of LDH layers. The excess enantiomer is (2*S*,1'*R*).

mainly at the edges of interlayer region or at the gallery entrances. For the catalysts giving visible enantioselective promotion, the fluorescent light was homogeneous throughout the hexagonal crystallite (Figure 6b and c), indicating that the catalysis took place homogeneously in the interlayer region. The observations further demonstrate the role of LDH layers in the enantioselectivity enhancement as huge and rigid planar substituent of attached chiral α -amino acid ligand.

To make full use of the LDH layer as a planar substituent of attached α -amino acid ligand, edge interlayer catalytic sites should be avoided. Our previous work^[24] has revealed that the location of vanadium centers could be controlled by changing the dosed quantity of vanadium sources. When less vanadium was dosed, vanadium centers were mainly coordinated to the amino acid ligand at edge interlayer sites before they diffused to the inner interlayer region. But for Zn^{II} centers, the alteration of Zn^{II} dosage does not work as expected probably because their diffusion to inner interlayer region seems to be inhibited more severely. So the location of Zn^{II} centers has been altered experimentally through ex-

foliating the ligand-intercalated LDHs or changing the Zn^{II} sources in this work. Exfoliation is able to increase the accessibility of ligand to Zn^{II} center, and neutral Zn^{II} sources could avoid the static repulsion between positively charged metal centers and brucite-like LDH layers.

Conclusion

The LDH layer has been revealed to act as an analogue to a planar substituent of a chiral ligand, for example, α -amino acid, to improve the enantioselectivity through both steric synergies and multiple H-bonding interactions when the active centers are located at the inner interlayer regions; its efficiency was investigated in the vanadium-catalyzed asymmetric epoxidation of allylic alcohols and the zinc-catalyzed direct asymmetric aldol addition between unmodified ketones and aldehydes. The main findings of this work are expected to highlight an efficient strategy for catalyst design in heterogeneous asymmetric synthesis. The planar substituent effect can be further expanded to other nanosheet materials.

Experimental Section

General procedure for the synthesis of L-glutamate intercalated LDHs:

The attachment of L-glutamate to brucite-like layers of LDHs was implemented by the ion exchange using Zn/Al-NO₃ as the precursor. The input Zn/Al molar ratio is ensured around 2:1. The chemical composition for the resulting intercalate is calculated as [Zn_{0.60}Al_{0.41}(OH)₂ (L-glutamate)_{0.17}(CO₃)_{0.05}·0.78H₂O according to the inductively coupled plasma (ICP) MS (Shimadzu ICPS-7500) and C, H, N (Bruker CHNS elemental analyzer) elemental analysis results. The XRD patterns of the resulting intercalated LDHs present characteristic diffractions of stacked layers. The basal spacing of L-glutamate intercalated LDHs is measured as 1.23 nm. The delamination of L-glutamate intercalated LDHs was achieved by abundant use of formamide.

General procedure for the catalytic asymmetric reaction: In a typical vanadium-catalyzed epoxidation, a catalytic amount of [VO(O-*i*Pr)₃] (0.0208 mmol) and ligand (equivalent to 0.0210 mmol of L-glutamate) was dispersed in CH₂Cl₂ (1 mL) and HCONH₂ (21 mL). After the reaction mixture was stirred for 1 h at 20 °C, anhydrous *tert*-butyl hydroperoxide (TBHP; 1.59 mmol) and 2-methyl cinnamyl alcohol (0.710 mmol) were added. The mixture was stirred at the same temperature for another 24 h. The reaction was monitored by TLC. Saturated aqueous Na₂SO₃ was used to quench the reaction, and the mixture was stirred for 1 h at 20 °C, then extracted with anhydrous ether. The ether phase was dried over Na₂SO₄, and concentrated under reduced pressure. The residue was purified by flash column chromatography on silica gel (eluent ethyl acetate/hexane = 1:2) to provide the epoxy alcohol. The assignment of the HPLC or GC retention time to the configuration of corresponding epoxy alcohol was made in reference to literature.^[31] In a typical zinc-catalyzed aldol reaction, a catalytic amount of Zn(OAc)₂ (0.011 mmol) and ligand (equivalent to 0.0165 mmol of L-glutamate) was added to cyclohexanone (4.0 mmol) and 4-nitrobenzaldehyde (0.055 mmol) in formamide (10 mL). The dosage of Zn^{II} is 20 mol% referring to the moles of 4-nitrobenzaldehyde, and the molar ratio of amino acid to zinc is 1.5:1 if not specially indicated. The mixture was stirred at 25 °C for 12 h. From the reaction mixture, a sample was taken (200 μ L) and poured into an extraction funnel containing brine (2 mL), diluted with distilled H₂O (2 mL), and EtOAc (2 mL). The aqueous phase was extracted with EtOAc (2 mL) twice. The combined organic phases were dried with Na₂SO₄ and concentrated under reduced pressure. The residue was dissolved in meth-

anol (1 mL) and subject to HPLC (Daciel Chiral AD-H column) for conversion and *ee* determinations. The assignment of the HPLC or GC retention time to the configuration of corresponding enantiomers was made in reference to literature.^[32] All data was reproduced at least twice.

Computational details: In this work, the H-bonding interactions between host layer and the multiple-guests were investigated by density functional theory (DFT)^[33] modeling with periodic boundary conditions of Zn/Al LDH layer. The Zn/Al molar ratio is taken as 2 in an ideal LDH layer with an *R3m* space group. The lattice parameter of the two-dimensional LDH layer is $a=b=3.02$ Å according to the X-ray diffraction (XRD) measurements.^[23] All geometries were fully optimized with Gaussian 09 package of programs (Revision B.01),^[34] and the basis set LANL2DZ^[35] was used for V, Zn, and Al, whereas 6-31G^[36] was used for the other atoms.

Acknowledgements

The authors wish to thank NSFC and 973 Project (2011CBA00504) for financial support. J.H. particularly appreciates the financial aid of the China National Funds for Distinguished Young Scientists from the NSFC.

- [1] J. M. Hawkins, T. J. N. Watson, *Angew. Chem.* **2004**, *116*, 3286–3290; *Angew. Chem. Int. Ed.* **2004**, *43*, 3224–3228.
- [2] M. Breuer, K. Ditrich, T. Habicher, B. Hauer, M. Keßeler, R. Stürmer, T. Zelinski, *Angew. Chem.* **2004**, *116*, 806–843; *Angew. Chem. Int. Ed.* **2004**, *43*, 788–824.
- [3] K. Soai, T. Shibata, I. Sato, *Acc. Chem. Res.* **2000**, *33*, 382–390.
- [4] H. F. Rase, *Handbook of Commercial Catalysts: Heterogeneous Catalysts*, CRC Press, New York, **2000**.
- [5] I. Vankelecom, A. Wolfson, S. Gresh, M. Landau, M. Gottlieb, M. Hershkovitz, *Chem. Commun.* **1999**, 2407–2408.
- [6] D. Pini, A. Mandoli, S. Orlandi, P. Salvadori, *Tetrahedron: Asymmetry* **1999**, *10*, 3883–3886.
- [7] R. Annunziata, M. Benaglia, M. Cinquini, F. Cozzi, M. Pitillo, *J. Org. Chem.* **2001**, *66*, 3160–3166.
- [8] J. M. Fraile, J. I. García, M. A. Harmer, C. I. Herrerías, J. A. Mayoral, *J. Mol. Catal. A: Chem.* **2001**, *165*, 211–218.
- [9] K. Hallman, C. Moberg, *Tetrahedron: Asymmetry* **2001**, *12*, 1475–1478.
- [10] M. Laspéras, N. Bellocq, D. Brunel, P. Moreau, *Tetrahedron: Asymmetry* **1998**, *9*, 3053–3059.
- [11] B. F. G. Johnson, S. A. Raynor, D. S. Shephard, T. Mashmeyer, J. M. Thomas, G. Sankar, S. Bromley, R. Oldroyd, L. Gladdenc, M. D. Mantle, *Chem. Commun.* **1999**, 1167–1168.
- [12] R. Raja, J. M. Thomas, *J. Mol. Catal. A: Chem.* **2002**, *181*, 3–14.
- [13] S. Xiang, Y. Zhang, Q. Xin, C. Li, *Chem. Commun.* **2002**, 2696–2697.
- [14] R. I. Kureshy, I. Ahmad, N. H. Khan, S. H. R. Abdi, S. Singh, P. H. Pandia, R. V. Jasra, *J. Catal.* **2005**, *235*, 28–34.
- [15] M. D. Jones, R. Raja, J. M. Thomas, B. F. G. Johnson, D. W. Lewis, J. Rouzaud, K. D. M. Harris, *Angew. Chem.* **2003**, *115*, 4462–4467; *Angew. Chem. Int. Ed.* **2003**, *42*, 4326–4331.
- [16] P. Yu, J. He, C. Guo, *Chem. Commun.* **2008**, 2355–2357.
- [17] P. Yu, J. He, C. Guo, L. Yang, M. Pu, X. Guo, *J. Catal.* **2008**, *260*, 81–85.
- [18] L. Zhao, X. Han, Y. Li, P. Yu, J. He, *ACS Catal.* **2012**, *2*, 1118–1126.
- [19] Z. An, W. Zhang, H. Shi, J. He, *J. Catal.* **2006**, *241*, 319–327.
- [20] J. M. Fraile, J. I. García, J. A. Mayoral, M. Roldán, *Org. Lett.* **2007**, *9*, 731–733.
- [21] J. I. García, B. López-Sánchez, J. A. Mayoral, E. Pires, I. Villalba, *J. Catal.* **2008**, *258*, 378–385.
- [22] H. Shi, C. Yu, J. He, *J. Catal.* **2010**, *271*, 79–87.
- [23] J. Wang, L. Zhao, H. Shi, J. He, *Angew. Chem. Int. Ed.* **2010**, *49*, 9171–9176.
- [24] L. Zhao, H. Shi, J. Wang, J. He, *Chem. Eur. J.* **2012**, *18*, 9911–9918.

- [25] C. Palomo, M. Oiarbide, J. M. García, *Chem. Soc. Rev.* **2004**, 33, 65–75.
- [26] T. D. Machajewski, C.-H. Wong, *Angew. Chem.* **2000**, 112, 1406–1430; *Angew. Chem. Int. Ed.* **2000**, 39, 1352–1375.
- [27] J. G. Hernández, E. Juaristi, *J. Org. Chem.* **2011**, 76, 1464–1467.
- [28] P. A. Kollman, L. C. Allen, *Chem. Rev.* **1972**, 72, 283–303.
- [29] L. Zhao, H. Shi, J. Wang, J. He, *Chem. Eur. J.* **2012**, 18, 15323–15329.
- [30] L. S. Sapochak, F. E. Benincasa, R. S. Schofield, J. L. Baker, K. K. C. Riccio, D. Fogarty, H. Kohlmann, K. F. Ferris, P. E. Burrows, *J. Am. Chem. Soc.* **2002**, 124, 6119–6125.
- [31] W. Zhang, A. Basak, Y. Kosugi, Y. Hoshino, H. Yamamoto, *Angew. Chem.* **2005**, 117, 4463–4465; *Angew. Chem. Int. Ed.* **2005**, 44, 4389–4391.
- [32] B.-L. Zheng, Q.-Z. Liu, C.-S. Guo, X.-L. Wang, L. He, *Org. Biomol. Chem.* **2007**, 5, 2913–2915.
- [33] C. Lee, W. Yang, R. G. Parr, *Phys. Rev. B* **1988**, 37, 785–789.
- [34] Gaussian 09, Revision B.01, M. J. Frisch, G. W. Trucks, H. B. Schlegel, G. E. Scuseria, M. A. Robb, J. R. Cheeseman, G. Scalmani, V. Barone, B. Mennucci, G. A. Petersson, H. Nakatsuji, M. Caricato, X. Li, H. P. Hratchian, A. F. Izmaylov, J. Bloino, G. Zheng, J. L. Sonnenberg, M. Hada, M. Ehara, K. Toyota, R. Fukuda, J. Hasegawa, M. Ishida, T. Nakajima, Y. Honda, O. Kitao, H. Nakai, T. Vreven, J. A. Montgomery, Jr., J. E. Peralta, F. Ogliaro, M. Bearpark, J. J. Heyd, E. Brothers, K. N. Kudin, V. N. Staroverov, R. Kobayashi, J. Normand, K. Raghavachari, A. Rendell, J. C. Burant, S. S. Iyengar, J. Tomasi, M. Cossi, N. Rega, J. M. Millam, M. Klene, J. E. Knox, J. B. Cross, V. Bakken, C. Adamo, J. Jaramillo, R. Gomperts, R. E. Stratmann, O. Yazyev, A. J. Austin, R. Cammi, C. Pomelli, J. W. Ochterski, R. L. Martin, K. Morokuma, V. G. Zakrzewski, G. A. Voth, P. Salvador, J. J. Dannenberg, S. Dapprich, A. D. Daniels, Ö. Farkas, J. B. Foresman, J. V. Ortiz, J. Cioslowski, D. J. Fox, Gaussian, Inc., Wallingford CT, **2010**.
- [35] J. B. Collins, P. v. R. Schleyer, J. S. Binkley, J. A. Pople, *J. Chem. Phys.* **1976**, 64, 5142–5151.
- [36] R. Ditchfield, W. J. Hehre, J. A. Pople, *J. Chem. Phys.* **1971**, 54, 724–728.

Received: March 26, 2013
Published online: July 23, 2013